Crack Identification in Beams Using Haar Wavelets and Machine Learning Methods

Ljubov Jaanuska, Helle Hein

***Abstract*—This article addresses a numerical identification of some characteristic parameters of cracks in a vibrating beam. The beam rests on Pasternak elastic foundation. The depth or location of crack(s) is predicted using the feedforward artificial neural networks or the random forest method. The machine learning methods are trained twice using two independent datasets based on the natural frequencies or the Haar wavelet transform of the first or third mode shapes. The approaches are compared to each other. The significance of the Haar wavelet transform and the random forest lies in their ability to make relatively fast parameter predictions; however, the complex approach of Haar wavelets and neural networks provides more precise results.**

***Index Terms*—open crack, elastic foundation, Haar wavelets, neural networks, random forest**

I. INTRODUCTION

THE soil-structure interaction problems play an important role in civil engineering (e.g. construction of pipelines, road surfaces, building foundations, etc.). Some of the problems (e.g. contact pressure distribution, buckling, cracks in the medium, etc.) can be idealized and solved by modeling a beam on an elastic foundation.

There are various models of beams on an elastic foundation described in literature, e.g. Winkler, Pasternak, Vlasov, Filonenko-Borodich, Leontiev models, etc; however, the first two models are widely used in engineering for the static and dynamic analysis of the beams resting on an elastic foundation for their simplicity. In Winkler one parameter model, the foundation is composed of infinitely close elastic springs which are independent of each other; the vertical surface displacement of the beam is assumed to be proportional to the contact pressure at any point [1]. Pasternak improved Winkler model by adding shear interactions. Pasternak two parameter model represents a system of closely placed elastic springs coupled to each other with elements which transmit the shear force proportional to the slope of the foundation surface [2].

The characteristic functions of the beam on an elastic foundation can be calculated using various numerical solutions. For instance, Providakis and Beskos studied the problem using the boundary element method [3]. Sheinman et al. obtained the axial displacements of the isotropic simply supported beams on an elastic foundation by the aid of the Rayleigh-Ritz procedure [4]. Chen applied the differential quadrature element method [5] . Yan et al. studied the dynamic response of functionally graded beams with an open crack resting on an elastic foundation using Hamilton's principle and Galerkin's method [6].

A large number of the numerical solutions are based on mesh methods, such as the finite element method [7], [8], the finite difference method [9], the spectral finite element method [10], etc. Such methods have some deficiencies related to the mesh definition, calculation and computer storage.

The aim of this paper is to focus on more time-efficient and less computationally intensive multidimensional mesh-free methods for predicting the characteristic parameters of cracks occurring in isotropic beams resting on an elastic foundation. For this reason, the machine learning approach has been chosen. Two the most outstanding methods are the back propagation artificial neural networks (ANNs) and the random forest (RF). Due to the flexibility and accuracy, the back propagation ANNs have been widely used in manifold areas of research since the determination of the ANN by Werbos in 1974 and rediscovery by Parker in 1985 and by Rumelhart and McClelland in 1986 [11]. In the field of structural mechanics and materials, Waszczyszyn and Ziemiański applied the ANNs to the following problem sets: simulation of physical relationship in case of bending of elastoplastic beams, neural simulation of return mapping algorithm for analysis of elastoplastic plane stress, estimation of fundamental vibration periods of real buildings, detection of damage in a steel beam and identification of loads applied to an elastoplastic beam. The ANNs produced robust and trustworthy results [12]. Chojaczyk provided an approbative review of ANNs and their applications in the structural reliability analysis of steel structures for the period 1989 and 2012; according to the author, the ANNs can be efficient alternatives to the traditional reliability methods for the analysis of complex structures [13]. Zhang and Subbarayan evaluated the ANNs for the optimal design of structural systems and confirmed that the advantage of the ANNs lies in the obviating the need for the exact function evaluations during the optimization, which is the main source of the computational expense during the optimal design of engineering systems [14]. Fang, et al. successfully applied the ANNs to the free vibration analysis and the structural damage detection (location and severity of crack damage) in the cantilever [15]. Unfortunately, no application of the back propagation ANNs to the cracked homogeneous beam resting on Pasternak foundation has been found in literature.

The RF is a decision-tree-based method, which was conceived as a simple and accurate method of classification and regression in 2001 [16]. Due to its youthhead, the RF has been adopted only to the researches connected to data mining, image analysis and applied statistics. Wu, et al. successfully

L. Jaanuska and H. Hein are with the Department of Computer Science, University of Tartu, J. Liivi 2, 50409, Tartu, Estonia. E-mail: ljubov.feklistova@ut.ee, helle.hein@ut.ee

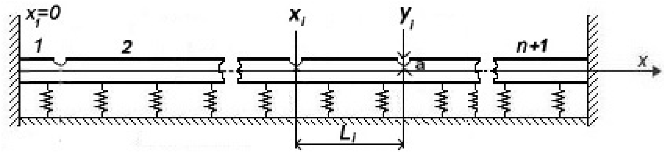

Fig. 1. Euler-Bernoulli beam on Pasternak foundation.

applied the RF to the study on imbalanced text categorization [17]. Calderoni, et al. developed a complex method for indoor localization using the RF classifiers [18]. Tüselmann, et al. described a new method based on the RF for determining journal rankings [19]. The results produced by the RF in various researches are trustworthy[20]. In the field of structural engineering, only a few papers on application of RF can be found. Sainlez and Heyen conducted performance monitoring of an industrial boiler in 2010 [21]. Tooke, et al. used the RF to predict the building ages [22]. Zhou, et al. applied the RF recursive feature elimination for damage detection in four-storey steal shear benchmark building model [23]. Nevertheless, a large number of papers address the inverse problems of structural mechanics by applying the predecessors of the RF, e.g. CART and C4.5 methods [24], [25], [26].

The main goals of the present paper are to identify the characteristic parameters of the crack(s) in the homogeneous beam resting on Pasternak elastic foundation using two different machine learning methods (the conventional ANNs and the most recent RF) and two different datasets (based on the natural frequencies and the Haar wavelet transform of the mode shapes), to compare the methods to each other and to verify the adaptability of the RF to the structural mechanics. The integrity and computational efficiency of the methods are demonstrated through a couple of case studies. Since the application of the interest falls into the low frequency region, the Euler-Bernoulli beam theory is chosen.

The present paper is organized in six sections. Section 2 describes the physical model. Section 3 introduces the RF method. Section 4 is devoted to the Haar wavelet transform. In Section 5, numerical examples are given. Finally, in Section 6 the conclusions and final remarks are drawn.

II. State Equations and Boundary Conditions

Consider an Euler-Bernoulli beam of length L with n cracks. The beam resting on Pasternak foundation has a rectangular cross-section, constant flexure rigidity EI and mass density m (Fig. 1).

According to the approach proposed by Rizos et al. [27] and Shifrin and Ruotolo [28], a beam can be divided into $n+1$ sections connected by springs; the springs represent n cracks. The differential equation of the transverse vibration in each region is

$$EI\frac{\partial^4 w_i(x_i,t)}{\partial x_i^4} - G_2\frac{\partial^2 w_i(x_i,t)}{\partial x_i^2} + G_1 w_i(x_i,t) + \\ + m\frac{\partial^2 w_i(x_i,t)}{\partial t^2} = 0, i = 1, ..., n+1, \tag{1}$$

where G_1 is the Winkler foundation modulus, G_2 is the shear modulus of Pasternak foundation, i is the number of the section and $w_i(x_i,t)$ is the transverse deflection. The solution of Eq.1 is sought in the form:

$$w_i(x_i,t) = W_i(x_i)sin(\omega t), \tag{2}$$

where $W_i(x_i)$ is the mode shape of the i-th beam section and ω is the natural frequency. Substituting Eq.2 into Eq.1, and introducing a variable:

$$\xi_i = \frac{x_i}{L_i} \tag{3}$$

the transverse vibration takes the form:

$$\frac{d^4 W_i(\xi_i)}{d\xi_i^4} - \mu_i\frac{d^2 W_i(\xi_i)}{d\xi_i^2} + (\gamma_i - \sigma_i)W_i(\xi_i) = 0, \tag{4}$$

where

$$\mu_i = \frac{G_2 L_i^2}{EI}, \gamma_i = \frac{G_1 L_i^4}{EI}, \sigma_i = \frac{m\omega^2 L_i^4}{EI}. \tag{5}$$

The characteristic equation of Eq.4 can be presented as:

$$\lambda^4 - \mu_i\lambda^2 + (\gamma_i - \sigma_i) = 0 \tag{6}$$

and the general solution of Eq.4 is

$$W_i = C_{1,i}e^{\lambda_1\xi_i} + C_{2,i}e^{\lambda_2\xi_i} + C_{3,i}e^{\lambda_3\xi_i} + C_{4,i}e^{\lambda_4\xi_i}, \tag{7}$$

where λ_1, ..., λ_4 are the roots of Eq.6 and $C_{1,i}$, ..., $C_{4,i}$ are the integration constants to be determined from the continuity and boundary conditions. The details of the different solutions are given by Rosa and Maurizi in [29].

Due to the localized crack effect, the beam with a crack of depth a_j at point y_j can be presented as two uniform beams joined together by massless linear spring at the crack. The bending constant of the spring is c_j [30]:

$$c_j = 5.346\frac{h}{EI}J(\eta_j), \eta_j = \frac{a_j}{h}, j = 1, ..., n, \tag{8}$$

where h is the height of the beam and $J(\eta_j)$ is the dimensionless local compliance function [30]:

$$J(\eta_j) = 1.8624(\eta_j)^2 - 3.95(\eta_j)^3 + 16.375(\eta_j)^4 - \\ - 37.226(\eta_j)^5 + 76.81(\eta_j)^6 - 126.9(\eta_j)^7 + \\ + 172(\eta_j)^8 - 143.97(\eta_j)^9 + 66.56(\eta_j)^{10}. \tag{9}$$

The continuity conditions at the crack y_j are expressed as following:

$$\begin{aligned} &W_j(y_j) = W_{j+1}(y_j) \\ &W_j''(y_j) = W_{j+1}''(y_j) \\ &W_j'''(y_j) = W_{j+1}'''(y_j) \\ &W_j'(y_j) + c_j W_j''(y_j) = W_{j+1}''(y_j), j = 1, 2, ..., n, \end{aligned} \tag{10}$$

where W_j and W_{j+1} are the mode shapes of the left and right beam sections, respectively.

In the present paper, a beam with clamped ends is investigated. The boundary conditions are as following:

$$W_1(0) = W_1^{'}(0) = 0,$$
$$W_{n+1}(1) = W_{n+1}^{'}(1) = 0. \tag{11}$$

Inserting Eq.7 into Eq.10 and Eq.11, the matrix equations are obtained. The natural frequencies are calculated by imposing zero value on the determinant of the coefficient matrix.

III. Random Forest

The random forest (RF) is a classifier defined by Breiman for the classification and regression problems. The statistical method is based on a large set of unpruned decision trees, which are known as classifiers. An unpruned tree, or a full tree, is a tree with many terminal nodes; each terminal node has minimal impurity and usually contains observations of one class only. A collection of the unpruned trees form an ensemble, or a forest.

The idea of combining multiple decision trees originated with Williams in 1988 [31]. Ho developed it further: for constructing each tree, he used a fixed portion of randomly selected features, or a subspace. The method is known as Random Decision Forest [32]. A bit later, Dietterich proposed the same idea of the random subspaces for constructing each node of the tree; in other words, to use a fixed portion of randomly selected features at each split of the node [33]. Finally, in 2001 Breiman formulated the whole RF algorithm as following [16]:

1) Generate n random sets of the observations (the bootstrap replicate sets) from the original set of the observations, where n is the number of trees in the ensemble. The size of each random set is the same as the size of the original set of the observations; however, in the bootstrap replicate set, the elements of the observation (predictor variables) are random: some variables are chosen several times from the original set, some are not at all. Each random set does not contain approximately 36 per cent of the original observation; these are called the "out-of-bag" observations.
2) Grow the forest of the unpruned classification or regression trees with minimum observations at each terminal node. For each tree, use the corresponding bootstrap set and recursively apply the following subalgorithm to construct a tree:
   a) choose random p predictor variables out of the original set (if p is equal to the size of the original set, the case is called bagging);
   b) choose a variable out of p which will produce the best split;
   c) split the set into two subsets at the node.

   Importantly, no pruning procedure can be applied after the tree has been fully built [34].
3) Evaluate each observation using all of the trees for which that observation is in the out-of-bag set. This produces an independent estimate of the classification error rate. The approach is similar to the use of separate training and test sets, or to N-fold cross validation [35].
4) Predict new observations by aggregating the predictions of each tree of the forest (i.e., majority votes for classification, average for regression).

Eventually, only a few parameters can be optimized in the RF: n - the number of trees (this parameter can be adjusted according to the evaluation based on out-of-bag sets); p - the number of the predictors used at each node (the smaller is p, the more reduced correlation is); the number of observations that the terminal nodes may contain (the default value can be one, which means the termimal nodes contain only observations of one class). The other parameters (the variables in the bootstrap sets and nodes) are random. The detailed guidance on adjusting these parameters can be found in [36].

The double randomness (at the generation of the bootsrap sets via bagging and the random subspaces at the nodes) decorrelates the trees in the ensamble allowing highly correlated variables to play almost equivalent roles. The decision based on the decisions from all of the classifiers increases the accuracy of the prediction made by one tree-structured classifier. This explains the efficiency and popularity of the RF in relation with other classification algorithms. The other advantages of the method are the impossibility of the overfitting and high computational efficiency due to the irrelevance of pruning, which is methodically and algorithmically laboriuos task.

In the present paper, in order to decorrelate the trees and increase the number of predictor variables in the sets from five to 32 without increase in the computational time, the Haar wavelet transform has been applied.

IV. Haar Wavelets

In the recent years, the wavelet transform has occasionally been implemented in structural health monitoring due to the fact that the wavelet transform does not require the analysis of the complete structure and has the ability to reveal some hidden parts of data that other signal analysis techniques fail to detect. Lepik [37] demonstrated that the Haar wavelets can be applied for the numerical solving of differential equations.

The Haar wavelet family is a group of square waves [37]:

$$h_i(x) = \begin{cases} 1 & for \quad x \in \left[\frac{k}{m}, \frac{2k+1}{2m}\right], \\ -1 & for \quad x \in \left[\frac{2k+1}{2m}, \frac{k+1}{m}\right], \\ 0 & elsewhere, \end{cases} \tag{12}$$

where m is the index of dilatation and it is equal to 2^j; j = 0,1,...,J indicates the level of the wavelet; k = 0,1,...,m-1 is the translation parameter. Integer J determines the maximal level of resolution. Index i is calculated according to the formula $i = m + k + 1$.

Proceeding from the definition above (Eq. 12), any function $y(x)$, which is square integrable in the interval [0,1], can be expanded into a Haar series with an infinite number of terms:

$$y(x) = \sum_{i=0}^{\infty} c_i h_i(x), \tag{13}$$

where the Haar coefficients are determined such that the integral square error ε is minimized

$$\varepsilon = \int_0^1 [y(x) - \sum_{i=1}^{m} c_i h_i(x)]^2 dx. \quad (14)$$

Any Haar function $h_i(x)$ can be calculated in the collocation points: $x_l = (l - 0.5)/2M$, where $l = 1, 2, \ldots, 2M$. The matrix $H(i, l) = h_i(x_l)$, which is associated with the Haar wavelets, is obtained as follows:

$$H(i,l) = \begin{vmatrix} h_1(x_1) & \ldots & h_1(x_{2M}) \\ \ldots & \ldots & \ldots \\ h_{2M}(x_1) & \ldots & h_{2M}(x_{2M}) \end{vmatrix} = H.$$

If the function $y(x)$ is a piece-wise constant or it can be approximated as a piece-wise constant, the sum is terminated as:

$$y(x_l) = \sum_{i=1}^{2M} c_i h_i(x) = c_{2M}^t h_{2M}, \quad (15)$$

where the coefficient vector is

$$c_{2M}^t = y_{2M}^* H_{2M\times 2M}^{-1} \quad (16)$$

and

$$y_{2M}^* = [y(1/4M)y(3/4M)...y((4M-1)/4M). \quad (17)$$

Both matrices H and H^{-1} are calculated once and contain zeros; therefore, the Haar transform works faster than Fourier transform.

V. Numerical Results

In the present paper, the depth or location of the crack(s) in the homogeneous beam resting on Pasternak elastic foundation were predicted using two different machine learning methods: the ANNs and the RF. For the training, three different datasets were calculated numerically: one was based on five natural frequencies and other two datasets were based on the Haar wavelet transform of the first or third mode shapes into 16 coefficients. Importantly, the test patters had not been shown to the systems in advance. In the tables, the average result of 100 runs and the relative error of the predictions are shown.

Example 1. In this case study, the depth of an open crack located in the middle of the vibrating clamped beam resting on Pasternak foundation ($G1$ = 100, $G2$ = 50) was investigated. The ratio of the height of the beam to the length was equal to 1/10. The depth of the crack was predicted by two approaches. In both methods, there were 106 training patterns and 10 test patterns in the dataset.

In Table I, the results are based on the feedforward back propagation ANN with one input, one output and one hidden layer with 20 neurons on it. The ANN was trained by Levenberg-Marquardt method; the elliot sigmoid was used as a transfer function. In Table I, the first column shows the numerically computed depth of the crack; column two present the results of the ANN trained by five natural frequencies; in the rest columns, the results which are based on the Haar wavelet transform into 16 coefficients. Importantly, in the last four columns, the Haar wavelet transform was based on the first and third mode shapes amplitude comparison [38]:

$$MSAC_q = \sum_{i=1}^{k} |W_{q,i}^u - W_{q,i}^d|, \quad (18)$$

where $W_{q,i}^u$ is the modal displacement for the i-th mode shape at coordinate q; u is the structure without any crack; d is the structure with a crack. In the present paper, the first and the third mode shapes were used because these contain more informative data [39].

The accuracy of predictions were estimated by calculating the relative error and the mean square error (MSE):

$$Relative\_error = \frac{\sqrt{(P_1-E_1)^2+(P_2-E_2)^2}}{\sqrt{(P_1^2+P_2^2)}}$$
$$MSE = \frac{1}{n}\sum(P-E)^2, \quad (19)$$

where P, P_1, P_2 are the predicted values, E, E_1, E_2 are the expected values and n is the number of test patterns.

TABLE I
Prediction of the depth of the crack in the beam resting on Pasternak foundation ($G1$ = 100, $G2$ = 50) using ANN.

Exact depth	Prediction based on five frequencies		Prediction based on the first mode shape and Haar transform into 16 coefficients	
Exact depth	Depth	Rel. err.	Depth	Rel. err.
0.0720	0.0720	0.0003	0.0721	0.0013
0.1160	0.1160	0.0002	0.1161	0.0008
0.1680	0.1678	0.0011	0.1682	0.0009
0.2040	0.2041	0.0004	0.2040	0.0001
0.2680	0.2680	0.0000	0.2682	0.0007
0.2960	0.2960	0.0001	0.2958	0.0007
0.3400	0.3406	0.0016	0.3404	0.0010
0.3840	0.3840	0.0000	0.3841	0.0004
0.4000	0.4000	0.0001	0.4000	0.0001
0.4680	0.4680	0.0001	0.4682	0.0004
MSE	4.10E-08		3.50E-08	

Exact depth	Prediction based on the third mode shape and Haar transform into 16 coefficients		Prediction based on the first and third mode shape and Haar transform into 16 coefficients	
Exact depth	Depth	Rel. err.	Depth	Rel. err.
0.0720	0.0725	0.0064	0.0715	0.0064
0.1160	0.1160	0.0003	0.1160	0.0004
0.1680	0.1682	0.0012	0.1679	0.0005
0.2040	0.2039	0.0004	0.2035	0.0024
0.2680	0.2674	0.0023	0.2681	0.0003
0.2960	0.2961	0.0004	0.2958	0.0006
0.3400	0.3402	0.0006	0.3395	0.0014
0.3840	0.3840	0.0001	0.3843	0.0009
0.4000	0.4000	0.0000	0.4001	0.0002
0.4680	0.4682	0.0003	0.4630	0.0108
MSE	7.50E-08		2.59E-05	

In Table II, the results are based on the RF and the same dataset as in the previous computation. To find the best values for n (the number of trees in the ensemble) and p (the number of the predictors at nodes) that can best predict the depth of the crack, the parameters were optimized based on the root mean square error and the out-of-bag estimation. The n values were tested from one to 50 with the interval of three, while p was tested from one to 32 using a single interval. In the case of the natural frequencies, the best results were obtained when there were fourteen trees in the ensemble, four predictors at the nodes and two observations at the terminal nodes (see Fig. 2); in case of the Haar wavelet transform, the best results were obtained when there were twelve trees in the ensemble, ten predictors at the nodes and one observation at the terminal nodes (see Fig. 3).

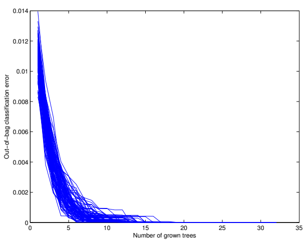

Fig. 2. Out-of-bag estimation for the RF trained by five frequencies.

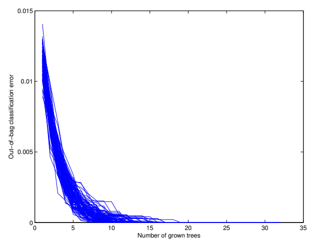

Fig. 3. Out-of-bag estimation for the RF trained by 16 coefficients.

TABLE II
PREDICTION OF THE DEPTH OF THE CRACK IN THE BEAM RESTING ON PASTERNAK FOUNDATION ($G1$ = 100, $G2$ = 50) USING RF.

Exact depth	Prediction based on five frequencies		Prediction based on the first mode shape and Haar transform into 16 coefficients	
Exact depth	Depth	Rel. err.	Depth	Rel. err.
0.0720	0.0699	0.0292	0.0707	0.0183
0.1160	0.1141	0.0164	0.1143	0.0150
0.1680	0.1659	0.0125	0.1671	0.0051
0.2040	0.2018	0.0108	0.2021	0.0092
0.2680	0.2667	0.0049	0.2683	0.0009
0.2960	0.2955	0.0017	0.2964	0.0015
0.3400	0.3395	0.0015	0.3426	0.0076
0.3840	0.3845	0.0013	0.3849	0.0023
0.4000	0.4005	0.0013	0.4008	0.0019
0.4680	0.4685	0.0011	0.4683	0.0007
MSE	2.02E-06		1.76E-06	

Exact depth	Prediction based on the third mode shape and Haar transform into 16 coefficients		Prediction based on the first and third mode shape and Haar transform into 16 coefficients	
Exact depth	Depth	Rel. err.	Depth	Rel. err.
0.0720	0.0726	0.0081	0.0701	0.0270
0.1160	0.1164	0.0037	0.1138	0.0187
0.1680	0.1682	0.0010	0.1660	0.0122
0.2040	0.2041	0.0006	0.2025	0.0075
0.2680	0.2667	0.0047	0.2678	0.0009
0.2960	0.2938	0.0073	0.2960	0.0001
0.3400	0.3405	0.0014	0.3403	0.0008
0.3840	0.3846	0.0015	0.3849	0.0024
0.4000	0.3992	0.0019	0.4002	0.0005
0.4680	0.4693	0.0028	0.4604	0.0163
MSE	1.00E-06		7.34E-06	

TABLE III
PREDICTION OF THE LOCATION OF TWO CRACKS IN THE BEAM RESTING ON PASTERNAK FOUNDATION ($G1$ = 10, $G2$ = 2.5 * π^2) USING ANN.

Exact locations of two cracks		Prediction based on five frequencies		
Crack 1	Crack 2	Crack 1	Crack 2	Rel. err.
0.1800	0.3700	0.3366	0.6809	0.8460
0.2100	0.4400	0.3886	0.6620	0.5844
0.2400	0.7900	0.2460	0.7546	0.0435
0.2700	0.7000	0.2848	0.7018	0.0199
0.3000	0.8500	0.2402	0.6448	0.2371
0.3300	0.4800	0.4048	0.5786	0.2125
0.3600	0.7100	0.3205	0.6508	0.0894
0.3900	0.6600	0.3590	0.6320	0.0545
0.4200	0.8100	0.3474	0.6373	0.2053
0.4500	0.6800	0.3701	0.5916	0.1461
0.4800	0.7100	0.3657	0.5679	0.2128
0.5100	0.7000	0.3677	0.5597	0.2307
0.5700	0.7200	0.3522	0.6131	0.2642
0.6600	0.8100	0.2897	0.6710	0.3786
MSE		0.0250	0.0255	

Exact locations of two cracks		Prediction based on the first mode shape and Haar transform into 16 coefficients		
Crack 1	Crack 2	Crack 1	Crack 2	Rel. err.
0.1800	0.3700	0.2487	0.4682	0.2913
0.2100	0.4400	0.3513	0.6091	0.4520
0.2400	0.7900	0.3094	0.7421	0.1021
0.2700	0.7000	0.2519	0.7193	0.0353
0.3000	0.8500	0.3495	0.8611	0.0563
0.3300	0.4800	0.3198	0.5476	0.1174
0.3600	0.7100	0.3342	0.6771	0.0525
0.3900	0.6600	0.3473	0.6492	0.0575
0.4200	0.8100	0.3904	0.7636	0.0603
0.4500	0.6800	0.4220	0.7389	0.0800
0.4800	0.7100	0.4939	0.7444	0.0433
0.5100	0.7000	0.4856	0.7067	0.0292
0.5700	0.7200	0.5379	0.7539	0.0508
0.6600	0.8100	0.4429	0.7343	0.2201
MSE		0.0062	0.0043	

Exact locations of two cracks		Prediction based on the first and third mode shape and Haar transform into 16 coefficients		
Crack 1	Crack 2	Crack 1	Crack 2	Rel. err.
0.1800	0.3700	0.1484	0.4822	0.2833
0.2100	0.4400	0.2322	0.4450	0.0467
0.2400	0.7900	0.2417	0.7805	0.0117
0.2700	0.7000	0.2815	0.6911	0.0194
0.3000	0.8500	0.3270	0.8046	0.0586
0.3300	0.4800	0.4199	0.5840	0.2360
0.3600	0.7100	0.3808	0.7040	0.0272
0.3900	0.6600	0.3844	0.6579	0.0078
0.4200	0.8100	0.3904	0.7942	0.0368
0.4500	0.6800	0.4371	0.6826	0.0161
0.4800	0.7100	0.4729	0.7152	0.0103
0.5100	0.7000	0.4756	0.6849	0.0434
0.5700	0.7200	0.5379	0.7036	0.0393
0.6600	0.8100	0.4703	0.8348	0.1831
MSE		0.0036	0.1524	

TABLE IV
PREDICTION OF THE LOCATION OF TWO CRACK IN THE BEAM RESTING ON PASTERNAK FOUNDATION ($G1$ = 10, $G2$ = 2.5 * π^2) USING RF.

Exact locations of two cracks		Prediction based on five frequencies		
Crack 1	Crack 2	Crack 1	Crack 2	Rel. err.
0.1800	0.3700	0.5056	0.7689	1.2514
0.2100	0.4400	0.3516	0.6679	0.5503
0.2400	0.7900	0.2256	0.7602	0.0401
0.2700	0.7000	0.2966	0.7106	0.0382
0.3000	0.8500	0.1814	0.6804	0.2296
0.3300	0.4800	0.4346	0.6025	0.2765
0.3600	0.7100	0.3122	0.6493	0.0971
0.3900	0.6600	0.3472	0.6183	0.0779
0.4200	0.8100	0.2884	0.5705	0.2995
0.4500	0.6800	0.3502	0.5820	0.1715
0.4800	0.7100	0.3324	0.5319	0.2699
0.5100	0.7000	0.3443	0.5237	0.2794
0.5700	0.7200	0.3380	0.5637	0.3046
0.6600	0.8100	0.2344	0.6064	0.4515
MSE		0.0392	0.0378	

Exact locations of two cracks		Prediction based on the first mode shape and Haar transform into 16 coefficients		
Crack 1	Crack 2	Crack 1	Crack 2	Rel. err.
0.1800	0.3700	0.2368	0.4054	0.1627
0.2100	0.4400	0.3530	0.5498	0.3698
0.2400	0.7900	0.2757	0.7361	0.0783
0.2700	0.7000	0.2640	0.7312	0.0423
0.3000	0.8500	0.2991	0.8132	0.0408
0.3300	0.4800	0.3337	0.6005	0.2070
0.3600	0.7100	0.3289	0.7272	0.0446
0.3900	0.6600	0.3666	0.6574	0.0307
0.4200	0.8100	0.3947	0.7541	0.0672
0.4500	0.6800	0.3588	0.7114	0.1183
0.4800	0.7100	0.4312	0.7057	0.0572
0.5100	0.7000	0.4618	0.6980	0.0557
0.5700	0.7200	0.4722	0.7321	0.1073
0.6600	0.8100	0.5464	0.7667	0.1164
MSE		0.0046	0.0030	

Exact locations of two cracks		Prediction based on the first and third mode shape and Haar transform into 16 coefficients		
Crack 1	Crack 2	Crack 1	Crack 2	Rel. err.
0.1800	0.3700	0.1799	0.4680	0.2382
0.2100	0.4400	0.2134	0.4463	0.0147
0.2400	0.7900	0.2732	0.7832	0.0410
0.2700	0.7000	0.2833	0.6644	0.0507
0.3000	0.8500	0.3854	0.8257	0.0985
0.3300	0.4800	0.3727	0.5702	0.1713
0.3600	0.7100	0.3892	0.7156	0.0373
0.3900	0.6600	0.3590	0.6297	0.0565
0.4200	0.8100	0.4072	0.8044	0.0153
0.4500	0.6800	0.4287	0.6374	0.0584
0.4800	0.7100	0.4659	0.6917	0.0270
0.5100	0.7000	0.4514	0.6890	0.0688
0.5700	0.7200	0.4972	0.7330	0.0805
0.6600	0.8100	0.4130	0.8117	0.2364
MSE		0.0057	0.0017	

Example 2. In this case study, the locations of two cracks in the scaled vibrating clamped beam resting on Pasternak foundation ($G1$ = 10, $G2$ = 2.5 * π^2) were predicted.

The depths of the cracks were equal to 2/10 of the beam height. The ratio of the height of the beam to the length was equal to 1/10. There were 130 training patterns and 14 test patterns in the dataset. For the ANN training, the same ANN was used as in the previous example. The average results based on the ANN training are shown in Table III. An attempt to add four hidden layers and create a five-layer diamond shaped ANN with 40, 60, 80, 60, 40 neurons on each layer did not give any good results; the relative error increased.

In case of the RF, the number of trees in the first forest was increased to 300 to predict the location of the first crack in the beam. In the second forest, there were 270 trees to predict the destination from the left end of the beam to the second crack. Also there were four predictors at the nodes and two observations at the terminal nodes. The average results of 100 runs are shown in Table IV.

VI. CONCLUSION

A complex approach of the ANN, the RF, the Haar wavelet transform and the natural frequencies is described in this paper for the localization of crack(s) in the homogeneous clamped beam resting on Pasternak elastic foundation. Both machine learning methods were similarly efficient and showed quite the same results; however, the RF worked faster and was easier to adjust. Moreover, the results were more precise if the machine learning methods were trained by the patterns obtained via the Haar wavelets transform of the first and third mode shapes; the second mode shape does not contain any useful information. Therefore, it is assumed the present research can serve as a good reference for future numerical research.

ACKNOWLEDGMENT

The authors would like to thank Estonian Research Council under Grant IUT 34-4.

REFERENCES

[1] Y. Ayvaz and K. Zgan, "Application of modified Vlasov model to free vibration analysis of beams resting on elastic foundations," *Journal of Sound and Vibration,* vol. 255, no. 1, pp. 111–127, 2002.

[2] Z. Celep, K. Gler and F. Demir, "Response of a completely free beam on a tensionless Pasternak foundation subjected to dynamic load," *Structural Engineering and Mechanics,* vol. 37, no. 1, pp. 61–77, 2010.

[3] C.P. Providakis and D.E. Beskos, "Dynamic analysis of beams by the boundary element method," *Computers & Structures,* vol. 22, no. 6, pp. 957–964, 1986.

[4] I. Sheinman, M. Adan and E. Altus, "On the role of the displacement function in nonlinear analysis of beams on an elastic foundation," *Thin-Walled Structures,* vol. 15, no. 2, pp. 109–125, 1993.

[5] C.-N. Chen, "Vibration of prismatic beam on an elastic foundation by the differential quadrature element method," *Computers & Structures,* vol. 77, no. 1, pp. 1–9, 2000.

[6] T. Yan, S. Kitipornchai, et al., "Dynamic behaviour of edge-cracked shear deformable functionally graded beams on an elastic foundation under a moving load," *Composite Structures,* vol. 93, no. 11, pp. 2992–3001, 2011.

[7] M. Skrinar and B. Lutar, "A three-node beam finite element for transversely cracked slender beams on Winkler's foundation," *Computational Materials Science,* vol. 64, pp. 260–264, 2012.

[8] Y.I. Özdemir, "Development of a higher order finite element on a Winkler foundation," *Finite Elements in Analysis and Design,* vol. 48, no. 1, pp. 1400–1408, 2012.

[9] R. Ansari, R. Gholami, K. Hosseini and S. Sahmani, "A sixth-order compact finite difference method for vibrational analysis of nanobeams embedded in an elastic medium based on nonlocal beam theory," *Mathematical and Computer Modelling,* vol. 54, no. 11–12, pp. 2577–2586, 2011.

[10] J. Li and H. Hua, "Spectral finite element analysis of elastically connected double-beam systems," *Finite Elements in Analysis and Design,* vol. 43, no. 15, pp. 1155–1168, 2007.

[11] V. Kecman, *Learning and Soft Computing: Support Vector Machines, Neural Networks, and Fuzzy Logic Models.* Cambridge, Mass.: MIT Press, 2001.

[12] Z. Waszczyszyn and L. Ziemiański, "Neural networks in mechanics of structures and materials - new results and prospects of applications," *Computers & Structures,* vol. 79, no. 22-25, pp. 2261–2276, 2001.

[13] A.A. Chojaczyk, A.P. Teixeira, L.C. Neves, et al., "Review and application of Artificial Neural Networks models in reliability analysis of steel structures," *Structural Safety,* vol.52, part A, pp. 78–89, 2015.

[14] L. Zhang and G. Subbarayan, "An evaluation of back-propagation neural networks for the optimal design of structural systems: Part I. Training procedures," *Computer Methods in Applied Mechanics and Engineering,* vol. 191, no. 25–26, pp. 2873–2886, 2002.

[15] X. Fang, H. Luo and J. Tang, "Structural damage detection using neural network with learning rate improvement," *Computers and Structures,* vol. 83, no. 25–26, pp. 2150–2161, 2005.

[16] L. Breiman, "Random forests," *Machine Learning*, vol. 45, pp. 5–32, 2001.

[17] Q. Wu, Y. Ye, H. Zhang, et al., "An efficient random forest algorithm for imbalanced text categorization," *Knowledge-Based Systems,* vol. 67, pp. 105–116, 2014.

[18] L. Calderoni, M. Ferrara, A. Franco, et al., "Indoor localization in a hospital environment using Random Forest classifiers," *Expert Systems with Applications,* vol. 42, no. 1, pp. 125–134, 2015.

[19] H. Tüselmann, R.R. Sinkovics and G. Pishchulov, "Towards a consolidation of worldwide journal rankings - A classification using random forests and aggregate rating via data envelopment analysis," *Omega,* vol. 51, pp. 11–23, 2015.

[20] M. Denil, D. Matheson and N. de Freitas, "Narrowing the gap: random forests in theory and in practice," *Proceedings of the 31st International Conference on Machine Learning*, vol. 32, pp. 403–408, 2014.

[21] M. Sainlez and G. Heyen, "Performance monitoring of an industrial boiler: classification of relevant variables with Random Forests," *Computer Aided Chemical Engineering,* vol. 28, pp. 403–408, 2010.

[22] T.R. Tooke, N.C. Coops and J. Webster, "Predicting building ages from LiDAR data with random forests for building energy modeling," *Energy and Buildings,* vol. 68, pp. 603–610, 2014.

[23] Q. Zhou, H. Zhou, Q. Zhou, et al., "Structure damage detection based on random forest recursive feature elimination," *Mechanical Systems and Signal Processing,* vol. 46, no. 1–3, pp. 82–90, 2014.

[24] W. Sun, J. Chen and J. Li, "Decision tree and PCA-based fault diagnosis of rotating machinery," *Mechanical Systems and Signal Processing,* vol. 21, no. 3, pp. 1300–1317, 2007.

[25] B.S. Yang, D.S. Lim and A.C.C. Tan, "VIBEX: an expert system for vibration fault diagnosis of rotating machinery using decision tree and decision table," *Expert Systems with Applications,* vol. 28, no. 4, pp. 735–742, 2005.

[26] A. Karbassi, B. Mohebi, S. Rezaee and P. Lestuzzi, "Damage prediction for regular reinforced concrete buildings using the decision tree algorithm," *Computers & Structures,* vol. 130, pp. 46–56, 2014.

[27] P.F. Rizos, N. Aspragathos and A.D. Dimarogonas, "Identification of crack location and magnitude in a cantilever beam from the vibration modes," *Journal of Sound and Vibration,* vol. 138, no. 3, pp. 381–388, 1990.

[28] E.I. Shifrin and R. Ruotolo, "Natural frequencies of a beam with arbitrary number of cracks," *Journal of Sound and Vibration*, vol. 222, no. 3, pp. 409–423, 1999.

[29] M.A. Rosa and M.J. Maurizi, "Dynamic analysis of multistep piles on Pasternak soil subjected to axial tip forces," *Journal of Sound and Vibration,* vol. 219, no. 5, pp. 771–783, 1999.

[30] S.A. Paipetis and A.D. Dimarogonas, "Analytical Methods in Rotor Dynamics," *Applied Science,* vol. 48, no. 1, 1986.

[31] G.J. Williams, "Combining decision trees: initial results from the MIL algorithm," on *Proc. Artificial Intelligence Developments and Applications: Selected papers from the first Australian Joint Artificial Intelligence Conference,*, Sydney, 1988, pp. 273–289.

[32] T.K. Ho, "Random decision forests," *Document Analysis and Recognition,* vol. 1, pp. 278–282, 1995.

[33] T. Dietterich, "An experimental comparison of three methods for constructing ensembles of decision trees: bagging, boosting, and randomization," *Machine Learning,* vol. 40, no. 2, pp. 139–157, 2000.

[34] S. del Río, V. López, J.M. Benítez and F. Herrera, "On the use of MapReduce for imbalanced big data using Random Forest," *Information Sciences,* vol. 285, pp. 112–137, 2014.

[35] M.H. Schwartz, A. Rozumalski, W. Truong and T.F. Novacheck, "Predicting the outcome of intramuscular psoas lengthening in children with cerebral palsy using preoperative gait data and the random forest algorithm," *Gait & Posture,* vol. 37, no. 4, pp. 473–479, 2013.

[36] A. Liaw, M. Wiener, "Classification and Regression by randomForest," *R News,* vol. 2, no. 3, pp. 18–22, 2002.

[37] U. Lepik, "Numerical solution of differential equations using Haar wavelets," *Mathematics and computers in simulation,* vol. 68, pp. 127–143, 2005.

[38] J.J. Sinou, "A review of damage detection and health monitoring of mechanical systems from changes in the measurement of linear and nonlinear vibrations," in *Mechanical Vibrations: Measurement, Effects and Control,*, R.C. Capri, Ed. Nova Science Publishers, Inc., 2009, pp. 643–702.

[39] J. Kullaa, "Distinguishing between sensor fault, structural damage, and environmental or operational effects in structural health monitoring," *Mechanical Systems and Signal Processing,*, vol. 25, no. 8, pp. 2976–2989, 2011.